

Stellar explosions, instabilities, and turbulence

R. P. Drake,¹ C. C. Kuranz,¹ A. R. Miles,² H. J. Muthsam,³ and T. Plewa⁴

¹University of Michigan, 2455 Hayward St., Ann Arbor, Michigan 48109, USA

²Lawrence Livermore National Laboratory, 7500 East Ave., Livermore, California 94550, USA

³Faculty of Mathematics, University of Vienna, Nordbergstr. 15, A-1090 Vienna, Austria

⁴School of Computational Science, Florida State University, DSL 443, Tallahassee, Florida 32306, USA

(Received 8 September 2008; accepted 12 December 2008; published online 22 April 2009)

It has become very clear that the evolution of structure during supernovae is centrally dependent on the pre-existing structure in the star. Modeling of the pre-existing structure has advanced significantly, leading to improved understanding and to a physically based assessment of the structure that will be present when a star explodes. It remains an open question whether low-mode asymmetries in the explosion process can produce the observed effects or whether the explosion mechanism somehow produces jets of material. In any event, the workhorse processes that produce structure in an exploding star are blast-wave driven instabilities. Laboratory experiments have explored these blast-wave-driven instabilities and specifically their dependence on initial conditions. Theoretical work has shown that the relative importance of Richtmyer–Meshkov and Rayleigh–Taylor instabilities varies with the initial conditions and does so in ways that can make sense of a range of astrophysical observations. © 2009 American Institute of Physics.

[DOI: [10.1063/1.3101816](https://doi.org/10.1063/1.3101816)]

I. INTRODUCTION

Stellar explosions involve the rapid release of energy within a star, whose pre-explosion structure sets the initial condition for the development of instabilities and perhaps turbulence during the explosion. The explosion deposits momentum in the stellar matter which in turn affects the longer-term evolution of the supernova (SN) event and the subsequent SN remnant. During the past 20 years, advances in observations have produced clear evidence of structure and asymmetry in stellar explosions, as evidenced specifically by SN 1987A,^{1,2} the Cassiopeia A (Cas A),^{3,4} and Tycho⁵ SN remnants, and more generally by spectropolarimetric evidence that asymmetric explosions are common.^{6–9} During the same period, advances in multidimensional simulations have led to modeling of stellar structure with an ever-increasing level of detail. This has included work to understand convection and magnetic-field generation in our sun and other stars, discussed below, and other works specifically aimed at pre-SN conditions, which we refer below. Modeling of core-collapse SNe has likewise advanced greatly, stimulated by clear evidence that explosions are typically asymmetric. Any SN explosion involves a blast wave created after energy is deposited deep within the star, which results in blast-wave-driven instability (BWI) evolution as the blast wave interacts with structure within the star. Experiments have recently begun to produce and explore BWI evolution relevant to the dynamics of core-collapse SNe. The combination of these elements has in turn motivated theoretical work that provides a useful context for interpretation of the results. This portion of the conference on high energy density laboratory astrophysics brought together recent work on stellar conditions, SNe of the core-collapse type, BWI experiments, and related theory.

II. STELLAR STRUCTURE

Stars contain convective zones because radiative energy transfer proves insufficient to transport the heat generated in the stellar core to the stellar surface, where it can be radiated away. Vigorous research has been performed on turbulent convection in the stellar case in recent years. Concentrating on normal, main sequence stars, the sun has been a major focus, one of the reasons being that truly detailed confrontations between observations and theory are feasible there. Such comparisons often deliver favorable results in the case of *solar granulation*, the outermost manifestation of the sun's convection zone. The very basic picture of granulation has been invariant since the early pioneering work of Nordlund:¹⁰ narrow cool downflow lanes border the broad hot updrafts and concentrate deeper down into downflowing plumes. Observations in more recent times increasingly hint toward a surface magnetic field different from the sun's general field, as for example in Ref. 11. Conceivably, this field is generated by a surface dynamo. While there have been contradicting results on the possibility of such a surface dynamo,^{12,13} recent work¹⁴ lends more credibility to this idea. The results surely have to do with the high numerical resolution used in that recent work. In the purely hydrodynamic case as well, resolution (and thus the degree of turbulence generated) is crucial. Such high-resolution runs (horizontal grid size of 10 km) show, for example, tubes of high vorticity in the stably stratified solar atmosphere, see Fig. 1. They are generated below in the turbulent convection zone and ascend subsequently. The pressure in the center of these tubes may be but one half of the ambient pressure, the tube being stabilized against collapse by strong centrifugal forces. These tubes sometimes arise as pairs with opposite sense of rotation of the constituents.

Modeling of whole *stellar convective envelopes* marks

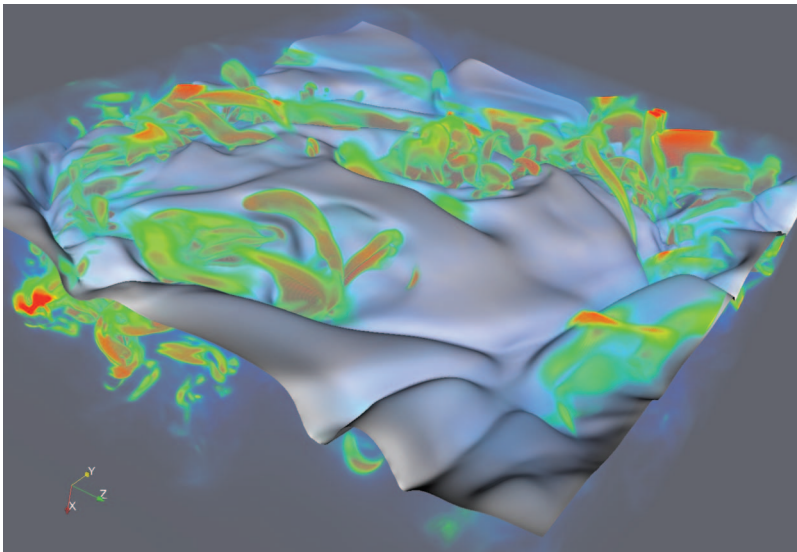


FIG. 1. (Color) High-resolution simulation of granular flows (horizontal grid size of 9.8 km). Isosurface: temperature (8000 K). Volume rendering: magnitude of $[\text{grad}(p) - \bar{p}]$, where p is the pressure and \bar{p} is horizontally averaged. Depth: 2.0 Mm; horizontal 4.1×3.9 Mm². For discussion see text.

the other main area. In the case of the sun, one issue is to match the rotational profiles as determined by helioseismology. Some important features are already reasonably reproduced, e.g., some aspects of the sun's differential rotation,¹⁵ which earlier, more laminar simulations did not correctly reproduce. Again, the generation of the solar magnetic field by a turbulent dynamo is at the center of interest. Current magnetohydrodynamic (MHD) models get some dynamo action.¹⁶ They fail, however, to obtain something as ordered as the solar magnetic field and cannot reproduce the solar magnetic cycle. This is ascribed in particular to the lack of a proper description of the shear layer near the bottom of the solar convection zone for want of resolution. This shear layer (tachocline) has been generally thought to be crucial for the operating of the solar dynamo, see Browning *et al.*¹⁷ for a study of tachocline effects. Therefore it comes as a surprise that even models of fully convective low mass stars (lacking any tachocline) now show magnetic fields with relatively large axisymmetric (ordered) components.¹⁸ While much still has to be done in order to elucidate even basic features, progress in modeling whole stellar convection zones is quite significant. There is also progress in modeling stellar convection in stars more relevant to core-collapse SNe,^{19–21} although these cases are not constrained by measurement in the way the solar models are. To a considerable degree, progress can be ascribed to the possibility to perform simulations in an increasingly turbulent regime, even if they are unable to resolve the actual degree of turbulence present in stars.

III. ASYMMETRIC IMPLOSIONS

Core-collapse (type II) SNe (Ref. 22) remain one of the longstanding problems of theoretical astrophysics. A great deal of observational data has been collected over the last several years and this trend is firmly expected to continue and strengthen. Recent observations revealed close connections between massive stars and gamma ray bursts, with the long gamma ray bursts seeming to be directly associated with core-collapse SN explosions.²³ These extreme events

are expected to be strongly asymmetric, producing highly collimated relativistic outflows, a property expected to be intimately linked to the central engine driving the explosion.²⁴

It is now widely believed that such asymmetries, although much milder and far smaller in scale, are in fact ubiquitous among core-collapse events.^{7–9} The best observed objects, Cas A and SN 1987A, actually provide direct evidence of intrinsic asymmetries. The Cas A SN remnant is famous for its jetlike emission features and highly structured distribution of heavy elements.⁴ It is not clear, however, whether the Cas A jets were produced by the central engine; an alternative, postexplosion mechanism has been proposed.²⁵ The situation is even less clear in case of SN 1987A. Observations clearly demonstrated that large scale mixing of chemical elements occurred very early on in the explosion.^{26–29} Furthermore, high resolution speckle observations revealed the presence of a very fast moving localized emission feature^{30–32} that could possibly be interpreted as a bidirectional ejection of material, perhaps a weak jet.³³

The origins of mixing and asymmetries in core-collapse SNe are undoubtedly deeply rooted in the explosion mecha-

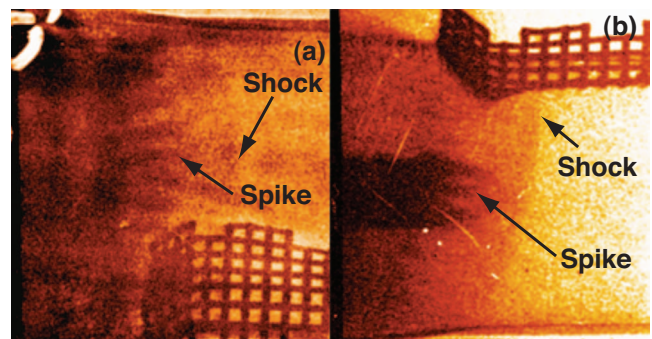


FIG. 2. (Color) These radiographic images are from an experiment performed using a target with a 3D, two mode initial pattern where the wavelength of the additional mode was $424 \mu\text{m}$. These images are two views of the same target where the views are orthogonal to each other. (a) is viewing the length of the tracer strip and (b) is viewing the width of the tracer strip. The target was imaged at 17 ns after the laser beams initially irradiated it.

nism. Without question rotation and magnetic fields may influence the morphology of the explosion and, in extreme cases, result in launching jets or highly collimated outflows.^{34–36} The role of pre-SN evolution is infrequently accounted for in modeling stellar explosions, but this may play an important role in the mixing process^{37,38} and evolution of the stalled accretion shock. Shock revival due to neutrino heating of the postshock layers remains a primary mechanism considered to be responsible for the explosion.^{39–41} However, so far successful explosion models have been obtained exclusively for relatively small masses of progenitors.⁴² With the computational demands of the core-collapse explosion problem being truly extreme, this field is bound to remain highly active for many years to come.

IV. RELEVANT LABORATORY EXPERIMENTS

In the specific case of core-collapse SNe, a shock is launched in the material that did not collapse inward, which soon evolves into a blast wave characterized by a shock front followed by a rarefaction. This blast wave is affected by density or velocity structure that it encounters, especially at the density transitions at composition interfaces. It steepens these density transitions and deposits vorticity at them, creating local regions where initial structures may grow due to Richtmyer–Meshkov (RM)^{43,44} processes, after which the structures will be further amplified as the steep transition decelerates by Rayleigh–Taylor (RT)^{45,46} instabilities. It has been shown that the local evolution near an interface is accurately described by the Euler equations, and laser-based laboratory experiments can produce conditions that are well scaled to those in the star over a finite region for a limited time.^{47,48} As is detailed in these references, the laboratory system and the SN both have very large Reynolds number, Peclet number, and radiation Peclet number, and both systems are sensibly described as fluids lacking phase transitions in the regime of interest. This implies that the same fluid equations describe both systems. In addition, the postshock structure at the unstable interfaces is shown to be very similar in the two cases. The postshock density jump in both cases corresponds to an Atwood number of about 2/3. This behavior has been explored in a sequence of experiments, marked by steadily increasing precision of the diagnostics and complexity of the structure.^{49–51} The potential for surprises exists in the high-Reynolds-number regime of these flows, which cannot be fully simulated, especially if fluid turbulence develops as the structures evolve.

The target for the experiments discussed at the conference is composed of two cylindrical layers of material within a shock tube. It has a 150 μm thick, denser layer of polyimide ($\text{C}_{22}\text{H}_{10}\text{O}_5\text{N}_2$) material into which the blast wave is launched, followed by a few millimeters of carbonized resorcinol formaldehyde foam. The densities of these materials are 1.43 g/cm^3 and 50 mg/cm^3 , respectively. A slot is machined into the center of the rear surface of the polyimide component. The slot is 75 μm thick, 230 μm wide, and the diameter of the polyimide piece is 905 μm . A strip of “tracer” material is glued into the slot. The tracer material is plastic doped with 4.3 at. % bromine and has a density of

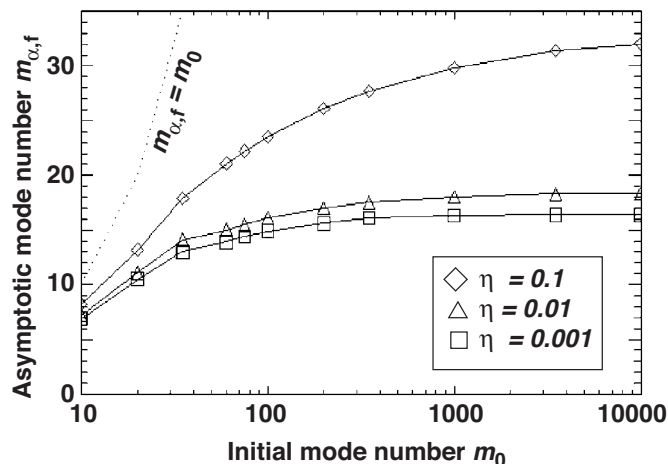


FIG. 3. Asymptotic characteristic mode number $m_{\alpha,f}$ vs initial mode number m_0 predicted by the BWI bubble-merger model. At high initial mode number, the interface structure loses its dependence on m_0 , signifying that memory of the initial conditions has been lost. When very low, the density ratio has only a weak effect on the asymptotic interface structure.

1.42 g/cm^3 . The purpose of this strip is to provide contrast in the x-ray radiographs obtained during the experiment. A seed perturbation is machined into the rear surface of the denser component. The experiments used several different perturbations, all including the same base pattern, which was a three-dimensional (3D) single mode having an amplitude of 2.5 μm and $k_x = k_y = 2\pi/(71 \mu\text{m})$, in which k_x and k_y are the wave numbers in two orthogonal directions along the surface of the interface. This single-mode pattern resembles an eggcrate. In two cases, this pattern is supplemented with additional modes to create a “multimode” pattern having additional long wavelength modes in one direction, either of 212 or 424 μm wavelength. In each case the maximum amplitude of the modulations is 2.5 μm .

5 kJ of laser energy irradiates the target in a 1 ns square pulse. The ablation pressure from the laser (~ 50 Mbars) causes a strong shock wave to traverse half of the polyimide layer before the laser pulse ends. The ablation pressure drops abruptly when the laser pulse ends, causing a rarefaction wave to move toward and eventually overtake the shock wave. This creates a blast-wave structure moving toward the interface between the plastic and the foam. The blast wave crosses the interface, first accelerating it and then decelerating it as the shock wave driven into the foam steadily accumulates mass. Any structure on the interface causes vorticity deposition by the shock front, creating a RM response. Subsequently, the density gradient across the interface opposes the pressure gradient in the blast wave, producing further growth of such structure by the RT instability. This experiment can observe the evolution of the interface until its deceleration becomes negligible.

This experiment is diagnosed by x-ray radiography using a pair of backlit pinholes to project signal from two x-ray sources onto x-ray film.⁵² The radiographs of Fig. 2, taken 17 ns after the laser beams irradiated the target, are from an experiment performed using a multimode perturbation, where the additional wavelength is 424 μm . The long fingers in the image are spikes due to the RT instability. In both

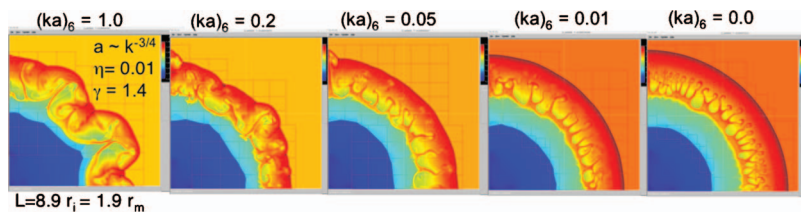


FIG. 4. (Color) Log density plots showing the effect of varying the degree of shock proximity by changing the initial amplitude in a series of RAPTOR BWI simulations seeded by low modes. At small initial amplitude, the RM contribution to the fast-phase growth is also small and the shock front is smooth. At about the threshold predicted by the planar strong shock relations and impulsive RM model ($ka_0=0.2$ for $\gamma=1.4$), the spikes extend to and perturb the shock front.

images the interface and the shock are moving to the right. The grid on the images is used as a spatial fiducial. [Fig. 2(a) is less distinct than Fig. 2(b) because additional postprocessing was needed to remove striations introduced by a filter used in that specific case.] Some features on these images do not correspond to data, including the thin, white streaks that are scratches on the film and the bright, white pixels in Fig. 2(b) that are flaws in the film. In Fig. 2(b) there are only three spikes visible and Fig. 2(a) has several more spikes. This difference is caused by the tracer strip. Figure 2(a) is viewing the length of the tracer strip and Fig. 2(b) is viewing only the width of the strip and therefore detects fewer spikes.

V. VARIABLE ROLE OF RAYLEIGH–TAYLOR AND RICHTMYER–MESHKOV MECHANISMS

BWI processes play a rich and varied role throughout the evolution of SNe from explosion to remnant, but interpreting their role is difficult due to the enormous complexity of the stellar systems. Insight can be gained by considering the simpler and fundamental hydrodynamic instability problem of a material interface between two constant-density fluids perturbed from spherical and driven by a divergent central Taylor–Sedov blast wave.⁵³ The existence of unified solutions⁵⁴ at high Mach number and small density ratio suggests that general conclusions can be drawn about the likely asymptotic structure of the mixing zone. To this end one can apply buoyancy drag^{55–58} and bubble merger models^{59,60} modified to include the effects of divergence and radial velocity gradients. In general, these effects preclude the true self-similar evolution⁶⁰ of classical Rayleigh–Taylor but can be incorporated into a quasiself-similar growth picture. Where the unified solution to the one-dimensional (1D) problem applies, multidimensional instability growth is not predicted to be strictly unified. Loss of memory of initial conditions can occur in the quasiself-similar model but requires initial mode numbers that are quite high. Despite the high-mode-number requirement for true loss of memory of initial conditions and the lack of strictly unified perturbation growth, the late-time asymptotic structure of the mixing zone is only weakly dependent on the initial conditions over a wide range of density ratios and initial perturbations. Figure 3 illustrates this for models evolving from an initial condition in which a high-pressure interior region of constant density expands against a region whose constant density is a factor of η times the initial interior density. Still, since very high modes are not dominant in the initial conditions predicted for type II SNe^{19,20,61} their late-time instability growth is likely influenced by details of the initial conditions.

Where large-amplitude modes are present in the initial conditions, the contribution to the perturbation growth from

the RM instability is significant or dominant compared to RT. The RM contribution will always be present where interface and transmitted shock are misaligned whether due to pre-transmission perturbations on the interface or the shock front. Such RM growth of large-amplitude low modes can yield proximity of the growing spikes to the forward shock and structure that strongly resemble that observed in the type IA Tycho⁵ remnant. Figure 4 illustrates this for a sequence of simulations using the code RAPTOR to model the system described above with reference to Fig. 3. In these simulations a spectrum of seed perturbations is present, with the perturbation of maximum amplitude having a product of wave number and amplitude given by $(ka)_6$ for a mode number of six, as indicated, and with the amplitude decreasing at higher wave number as $k^{-3/4}$. Here the polytropic index is γ , the density ratio η is 0.01, the initial radius of the interior region is r_i , the radius where the swept-up mass equals the interior mass is r_m , and L is the size of the computational domain equal to $8.9r_i$ and to $1.9r_m$. Initial conditions required to produce the observed structure might naturally arise following a deflagration to detonation transition.^{62,63} Thus, large-amplitude low-mode RM can potentially resolve the current discrepancy^{64,65} between the shock-interface structure observed in Tycho and numerical simulations.

VI. CONCLUSION

One can see in this recent work elements of convergence among modeling of stellar convection, stellar explosions, laboratory experiments, and fundamental theory. Improved understanding of stellar convection will improve the accuracy of initial conditions used in modeling of stellar explosions and in laboratory experiments on BWIs. Formulation of such models and experiments would do well to be informed by viewing observations in the context of the recent theoretical understanding that the initial conditions affect the relative dominance of RM as opposed to RT growth during stellar explosions.

ACKNOWLEDGMENTS

Work at the University of Michigan was sponsored by the National Nuclear Security Administration under the Stewardship Science Academic Alliances program through DOE Research Grant Nos. DE-FG52-07NA28058, DE-FG52-04NA00064, and other grants and contracts. The work of H.M. was supported by the Austrian Science Foundation, Project Nos. 18224 and P20762.

- ¹W. D. Arnett, J. N. Bahcall, R. P. Kirshner, and S. E. Woolsey, *Annu. Rev. Astron. Astrophys.* **27**, 629 (1989).
- ²R. A. Chevalier, *Nature (London)* **355**, 691 (1992).
- ³J. I. Reed, J. J. Hester, A. C. Fabian, and P. F. Winkler, *Astrophys. J.* **440**, 706 (1995).
- ⁴U. Hwang, S. S. Holt, and R. Petre, *Astrophys. J. Lett.* **537**, L119 (2000).
- ⁵U. Hwang, R. Petre, A. E. Szymkowiak, and S. S. Holt, *J. Astrophys. Astron.* **23**, 81 (2002).
- ⁶L. Wang, D. A. Howell, P. Höflich, and J. C. Wheeler, *Astrophys. J.* **550**, 1030 (2001).
- ⁷D. J. Jeffery, *Astrophys. J., Suppl. Ser.* **77**, 405 (1991).
- ⁸L. F. Wang, D. Baade, P. Höflich, and J. C. Wheeler, *Astrophys. J.* **592**, 457 (2003).
- ⁹D. C. Leonard, A. V. Filippenko, M. Ganeshalingam, F. J. D. Serduke, W. D. Li, B. J. Swift, A. Gal-Yam, R. J. Foley, D. B. Fox, S. Park, J. L. Hoffman, and D. S. Wong, *Nature (London)* **440**, 505 (2006).
- ¹⁰A. Nordlund, *Astron. Astrophys.* **107**, 1 (1982).
- ¹¹J. T. Bueno, N. Shchukina, and A. A. Ramos, *Nature (London)* **430**, 326 (2004).
- ¹²F. Cattaneo, T. Emonet, and N. Weiss, *Astrophys. J.* **588**, 1183 (2003).
- ¹³R. F. Stein and A. Nordlund, in *IAU Symposium 210*, edited by N. Piskunov, W. W. Weiss, and D. F. Gray (Astronomical Society of the Pacific, San Francisco, 2003), pp. 169.
- ¹⁴A. Vogler and M. Schussler, *Astron. Astrophys.* **465**, L43 (2007).
- ¹⁵A. S. Brun and J. Toomre, *Astrophys. J.* **570**, 865 (2002).
- ¹⁶A. S. Brun, M. S. Miesch, and J. Toomre, *Astrophys. J.* **614**, 1073 (2004).
- ¹⁷M. K. Browning, M. S. Miesch, A. S. Brun, and J. Toomre, *Astrophys. J. Lett.* **648**, L157 (2006).
- ¹⁸M. K. Browning, *Astrophys. J.* **676**, 1262 (2008).
- ¹⁹C. A. Meakin and D. Arnett, *Astrophys. J. Lett.* **637**, L53 (2006).
- ²⁰C. A. Meakin and D. Arnett, *Astrophys. J.* **667**, 448 (2007).
- ²¹C. A. Meakin and D. Arnett, *Astrophys. J.* **665**, 690 (2007).
- ²²A. V. Filippenko, *Annu. Rev. Astron. Astrophys.* **35**, 309 (1997).
- ²³J. C. Wheeler, *Phys. Plasmas* **13**, 058101 (2006).
- ²⁴P. Höflich, P. Kumar, and J. C. Wheeler, *Cosmic Explosions in Three Dimensions: Asymmetries in Supernovae and Gamma Ray Bursts* (Cambridge University Press, Cambridge, 2004).
- ²⁵A. R. Bell, *Mon. Not. R. Astron. Soc.* **385**, 1884 (2008).
- ²⁶R. W. Hatuschik and J. Dachs, *Astron. Astrophys.* **182**, L29 (1987).
- ²⁷R. W. Hatuschik, *Rev. Mod. Astron.* **4**, 233 (1991).
- ²⁸M. M. Phillips and S. R. Heathcote, *Publ. Astron. Soc. Pac.* **101**, 137 (1989).
- ²⁹V. P. Utrobin, *Astron. Lett.* **31**, 806 (2005).
- ³⁰W. P. S. Meikle, S. J. Matcher, and B. L. Morgan, *Nature (London)* **329**, 608 (1987).
- ³¹P. Nisenson, C. Papaliolios, M. Karovska, and R. Noyes, *Astrophys. J., Lett. Ed.* **320**, L15 (1987).
- ³²P. Nisenson and C. Papaliolios, *Astrophys. J. Lett.* **518**, L29 (1999).
- ³³L. Wang, J. C. Wheeler, P. Höflich, A. Khokhlov, D. Baade, D. Branch, P. Challis, A. V. Filippenko, C. Fransson, P. Garnavich, R. P. Kirshner, P. Lundqvist, R. McCray, N. Panagia, C. S. J. Pun, M. M. Phillips, G. Sonneborn, and N. B. Suntzeff, *Astrophys. J.* **579**, 671 (2002).
- ³⁴S. Akiyama, J. C. Wheeler, D. L. Meier, and I. Lichtenstadt, *Astrophys. J.* **584**, 954 (2003).
- ³⁵A. M. Khokhlov, P. F. Höflich, E. S. Oran, J. C. Wheeler and L. Wang, *Astrophys. J. Lett.* **524**, L107 (1999).
- ³⁶L. Dessart, A. Burrows, E. Livne, and C. D. Ott, *Astrophys. J. Lett.* **673**, L43 (2008).
- ³⁷P. Podsiadlowski, *Publ. Astron. Soc. Pac.* **104**, 717 (1992).
- ³⁸P. A. Young, C. Meakin, D. Arnett, and C. L. Fryer, *Astrophys. J. Lett.* **629**, L101 (2005).
- ³⁹M. Herant, *Phys. Rep.* **256**, 117 (1995).
- ⁴⁰L. Scheck, T. Plewa, H.-T. Janka, K. Kifonidis, and E. Mueller, *Phys. Rev. Lett.* **92**, 011103 (2004).
- ⁴¹A. Burrows, E. Livne, L. Dessart, C. D. Ott, and J. Murphy, *Astrophys. J.* **640**, 878 (2006).
- ⁴²R. Buras, H. T. Janka, M. Rampp, and K. Kifonidis, *Astron. Astrophys.* **457**, 281 (2006).
- ⁴³R. D. Richtmyer, *Commun. Pure Appl. Math.* **13**, 297 (1960).
- ⁴⁴E. E. Meshkov, *Soviet Fluid Dyn.* **4**, 101 (1969).
- ⁴⁵L. Rayleigh, *Scientific Papers II* (Cambridge University Press, Cambridge, 1900).
- ⁴⁶S. G. Taylor, *Proc. R. Soc. London* **A201**, 192 (1950).
- ⁴⁷D. D. Ryutov, R. P. Drake, J. Kane, E. Liang, B. A. Remington, and M. Wood-Vasey, *Astrophys. J.* **518**, 821 (1999).
- ⁴⁸D. D. Ryutov, R. P. Drake, and B. A. Remington, *Astrophys. J., Suppl. Ser.* **127**, 465 (2000).
- ⁴⁹R. P. Drake, D. R. Leibbrandt, E. C. Harding, C. C. Kuranz, M. A. Blackburn, H. F. Robey, B. A. Remington, M. J. Edwards, A. R. Miles, T. S. Perry, R. Wallace, H. Louis, J. Knauer, and D. Arnett, *Phys. Plasmas* **11**, 2829 (2004).
- ⁵⁰J. Kane, D. Arnett, B. A. Remington, S. G. Glendinning, J. Castor, R. Wallace, A. Rubenchik, and B. A. Fryxell, *Astrophys. J. Lett.* **478**, L75 (1997).
- ⁵¹H. F. Robey, J. O. Kane, B. A. Remington, R. P. Drake, O. A. Hurricane, H. Louis, R. J. Wallace, J. Knauer, P. Keiter, D. Arnett, and D. D. Ryutov, *Phys. Plasmas* **8**, 2446 (2001).
- ⁵²C. C. Kuranz, B. E. Blue, R. P. Drake, H. F. Robey, J. F. Hansen, J. P. Knauer, M. J. Grosskopf, C. Krauland, and D. C. Marion, *Rev. Sci. Instrum.* **77**, 10E327 (2006).
- ⁵³A. R. Miles, "The blast-wave-driven instability as a vehicle for understanding supernova explosion structure," *Astrophys. J.* (in press).
- ⁵⁴J. K. Truelove and C. F. McKee, *Astrophys. J., Suppl.* **120**, 299 (1999).
- ⁵⁵R. M. Davies and G. I. Taylor, *Proc. R. Soc. London, Ser. A* **200**, 375 (1950).
- ⁵⁶G. Dimonte and M. Schneider, *Phys. Rev. E* **54**, 3740 (1996).
- ⁵⁷J. C. V. Hansom, P. A. Rosen, T. J. Goldack, K. Oades, P. Fieldhouse, N. Cowperthwaite, D. L. Youngs, N. Mawhinney, and A. J. Baxter, *Laser Part. Beams* **8**, 51 (1990).
- ⁵⁸D. Oron, L. Arazi, D. Kartoon, A. Rikanati, U. Alon, and D. Shvarts, *Phys. Plasmas* **8**, 2883 (2001).
- ⁵⁹J. Glimm and X. L. Li, *Phys. Fluids* **31**, 2077 (1988).
- ⁶⁰D. H. Sharp, *Physica D* **12**, 3 (1984).
- ⁶¹K. Kifonidis, T. Plewa, H.-T. Janka, and E. Muller, *Astron. Astrophys.* **408**, 621 (2003).
- ⁶²A. M. Khokhlov, *Astron. Astrophys.* **245**, 114 (1991).
- ⁶³V. N. Gamezo, A. M. Khokhlov, and E. S. Oran, *Astrophys. J.* **623**, 337 (2005).
- ⁶⁴V. V. Dwarkadas, *Astrophys. J.* **541**, 418 (2000).
- ⁶⁵C. Y. Wang and R. A. Chevalier, *Astrophys. J.* **549**, 1119 (2001).